

# Dynamic monitoring of a bi-enzymatic reaction at a single biomimetic giant vesicle

Pauline Lefrançois, Bertrand Goudeau, Stéphane Arbault\*

Univ. Bordeaux, CNRS, Bordeaux INP, ISM, UMR 5255, F-33400, Talence, France.

## ELECTRONIC SUPPLEMENTARY INFORMATION

In the following are presented some supplementary results: 1. an imaging of the tip of the micropipettes prepared and used for single vesicle injections; 2. kinetic studies of the bi-enzymatic assay performed in bulk by conventional fluorescence spectroscopy; 3. control experiments dealing with the permeability of vesicle membranes as function of the fluorophore used; 4. exponential decay fittings of figures 3 to 6 demonstrating the low effect of photobleaching on the signal; 5. the dependence on Amplex Red concentration of the bi-enzymatic reaction efficiency in GUVs; 6. volumes and concentrations calculations for each injection and each experiment.

## 1. Micropipette variability

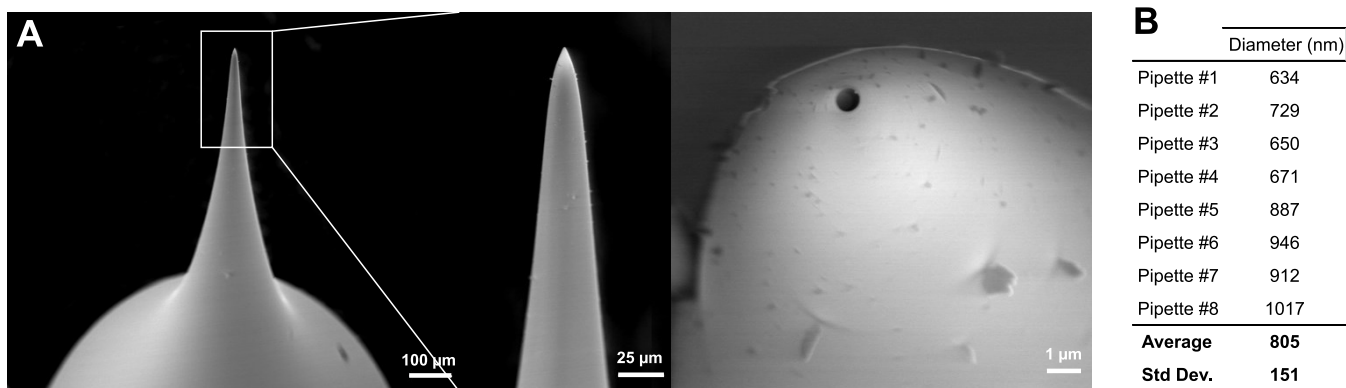


**Figure S1.** A. High resolution scanning electron microscope images of a typical micropipette used in the experiments, at 3 various scales (Nova NanoSEM 650, FEI – low vacuum detector). B. Micropipette opening tip diameters measured from SEM images for 8 samples. The average hole diameter was calculated as  $805 \pm 151$  nm, highlighting the variability of the micropipette sizes, which induces some adaptation in the microinjection duration-volume for each experiment.

## 2. Bulk kinetic study of the bi-enzymatic assay by fluorescence spectroscopy

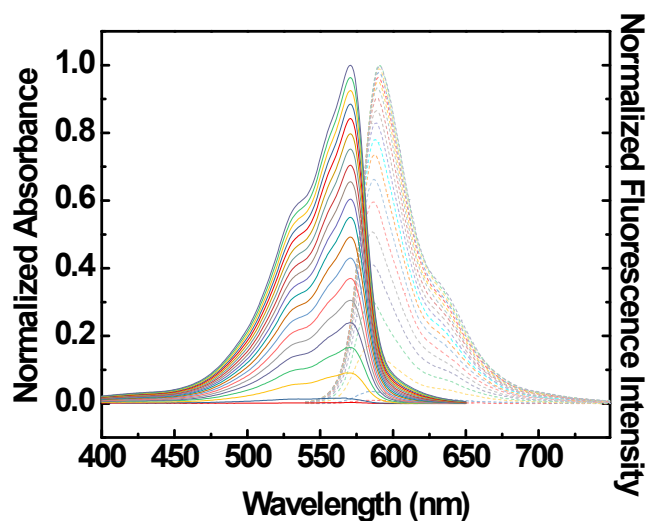


**Figure S2.** Normalized absorbance and fluorescence emission spectra of resorufin produced over time by the bi-enzymatic reaction coupling the GOx and HRP enzymatic reactions. The measurements were done in a cuvette in a UV-visible spectrophotometer (Cary 100, Varian) for the absorbance measurement and in a spectrofluorimeter (Cary Eclipse, Varian) for the emission measurement at the rate of 1 scan per 30 s. 100  $\mu\text{M}$  glucose, 50  $\mu\text{M}$  Amplex Red, 1  $\text{U}\cdot\text{mL}^{-1}$  GOx, 0.2  $\text{U}\cdot\text{mL}^{-1}$  HRP were used.

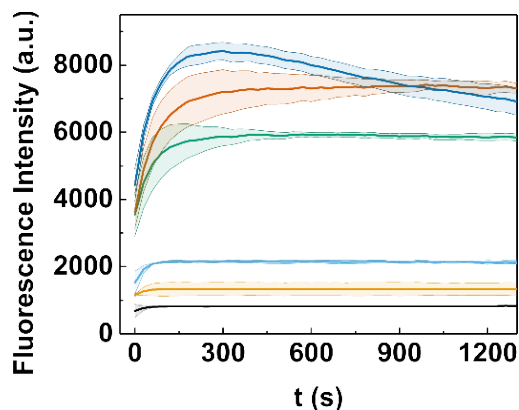


**Figure S3.** Fluorescence intensity of resorufin over time produced by the oxidation of Amplex Red (50  $\mu\text{M}$ ), catalysed by HRP (0.4  $\text{U}\cdot\text{mL}^{-1}$ ), for various concentration of hydrogen peroxide (Black: 1  $\mu\text{M}$ , Yellow: 2.5  $\mu\text{M}$ , Light blue: 5  $\mu\text{M}$ , Green: 20  $\mu\text{M}$ , Orange: 35  $\mu\text{M}$ , Dark blue: 50  $\mu\text{M}$ ). The measurement was done with a plate reader spectrophotometer (Spectra Max M2e, Molecular Devices) at  $\lambda_{\text{excitation}} = 488 \text{ nm}$  and  $\lambda_{\text{emission}} = 587 \text{ nm}$ . The measurement was repeated 3 times per condition. The 3 measurements were averaged (solid line) and the standard deviation is represented as a filled error plot. From 50  $\mu\text{M}$  the signal dropped after 5 min, possibly due to the oxidation of resorufin to resazurin<sup>3</sup>.

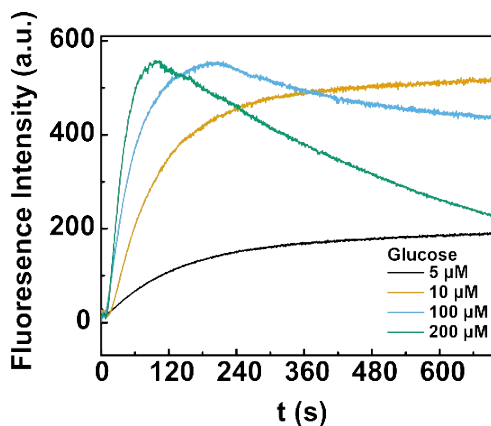


**Figure S4.** Fluorescence intensity of resorufin over time produced by the bienzymatic reaction. Glucose (at various concentrations) was oxidized via glucose oxidase catalysis (5  $\text{U}\cdot\text{mL}^{-1}$ ). Amplex Red (50  $\mu\text{M}$ ) was then oxidized to resorufin, catalysed by HRP (0.4  $\text{U}\cdot\text{mL}^{-1}$ ). The measurement was done at  $\lambda_{\text{excitation}} = 500 \text{ nm}$  for  $\lambda_{\text{emission}} = 660 \text{ nm}$  in a cuvette in a spectrofluorimeter (Cary Eclipse, Varian). The excitation and emission wavelengths were not set at the maximum of absorbance (572 nm) and emission (583 nm) to avoid saturation of the detector. The fluorescence decrease observed after  $\sim 120 \text{ s}$  on the blue and green traces may result from oxidation of resorufin (highly fluorescent) to resazurin (very low fluorescence) due to the remaining hydrogen peroxide production occurring after the AR runoff.

### 3. Control experiments

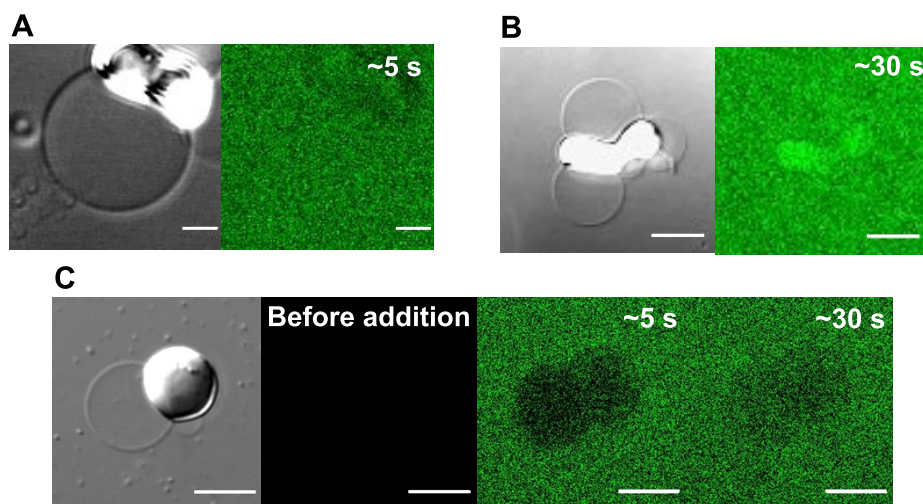


**Figure S5.** Negative contrast experiments were used to control whether the diffusion of resorufin across the membrane of GUVs was due to the microinjection and/or the application of electric pulse. GUVs were grown in PBS. After 15-20 min, a fluorophore solution was gently mixed to the solution containing the GUV (directly on the stage of the microscope). Images were obtained by laser scanning confocal microscopy (LSCM). A. resorufin (50  $\mu\text{M}$  final), imaging settings:  $\lambda_{\text{excitation}} = 514 \text{ nm}$  and  $\lambda_{\text{emission}} = 550\text{-}710 \text{ nm}$ ; B. fluorescein (50  $\mu\text{M}$  final), imaging settings:  $\lambda_{\text{excitation}} = 458 \text{ nm}$  and  $\lambda_{\text{emission}} = 480\text{-}630 \text{ nm}$ ; C. calcein (25  $\mu\text{M}$  final), imaging settings:  $\lambda_{\text{excitation}} = 514 \text{ nm}$  and  $\lambda_{\text{emission}} = 530\text{-}630 \text{ nm}$ . Scale bar: 20  $\mu\text{m}$ .

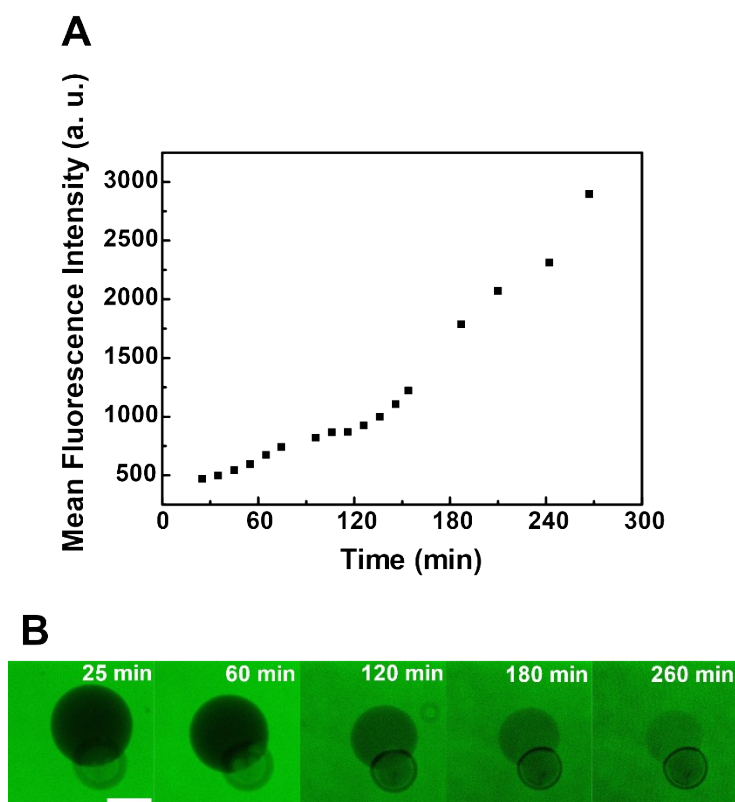


**Figure S6.** Negative contrast experiments. GUVs were grown in PBS. After 15-20 min, a Dextran-FITC 70 kDa solution (0.3  $\text{mg}\cdot\text{mL}^{-1}$  final) was gently mixed to the solution containing the GUV (directly on the stage of the microscope). Images were obtained by laser scanning confocal microscopy. A. The mean

fluorescence intensity inside the GUV is displayed over time. B. Microscopy time-lapse images obtained by LSCM showing the fluorescence increase inside the GUV over time. One may note that the GUV size slightly reduces over time, due to the total duration of this experiment (> 4h on a microscopy slide). Imaging settings:  $\lambda_{\text{excitation}} = 496 \text{ nm}$  and  $\lambda_{\text{emission}} = 510\text{-}660 \text{ nm}$ . Time interval: 30 s from 25 to 150 min, and 30 min from 150 to 260 min. Scale bar: 50  $\mu\text{m}$ .

#### 4. Analyses of fluorescence intensity decays demonstrating the low effect of photobleaching

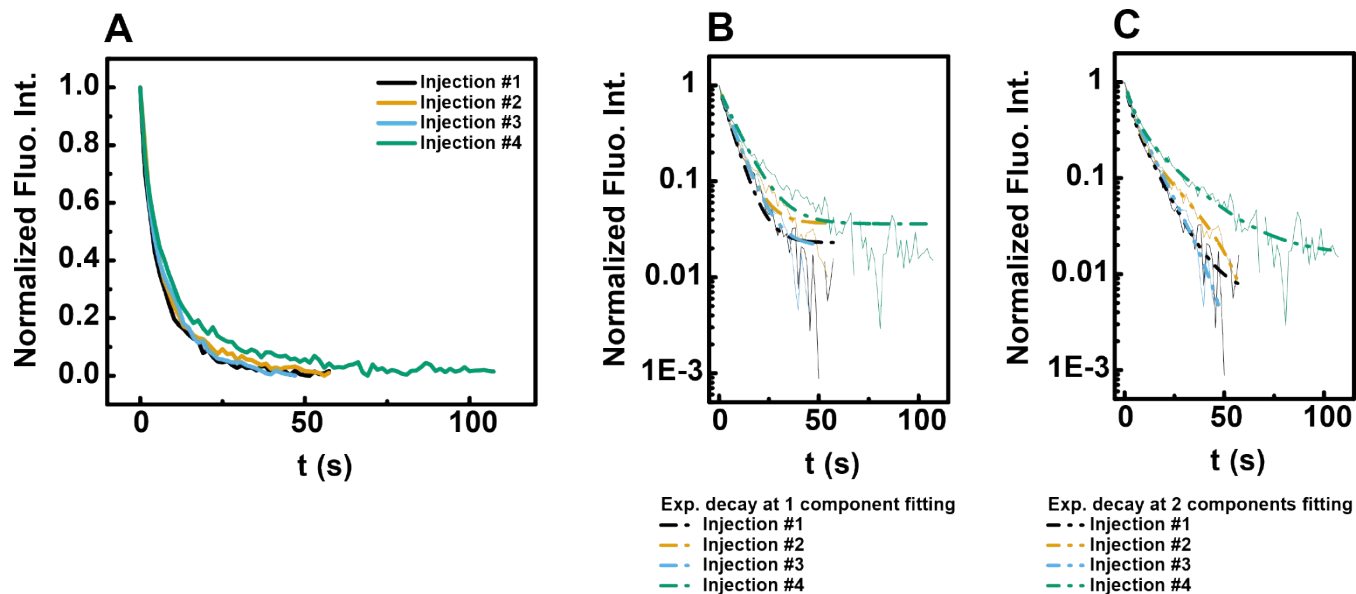


**Figure S7.** The signals of each injection from Figure 3 were normalized ([0;1]) and the x-axis was offset to  $t = 0$  for each injection (A). An exponential decay at 1 component fitting (B) and an exponential decay at 2 components fitting (C) were applied on each injection signal. B and C y-axis are in Log10. Solid lines represent the normalized fluorescence intensity of each injection. Dash-dot lines represent the exponential decay at 1 component fitting ( $y = A_1 \times \exp(-t/\tau_1) + y_0$ ). Dash-dot-dot lines represent the exponential decay at 2 components fitting ( $y = A_1 \times \exp(-t/\tau_1) + A_2 \times \exp(-t/\tau_2) + y_0$ ). The best fitting function of the signal is the 2-component exponential decay function. This shows the signal is composed of 2 contributions: 1/ the diffusion of resorufin and 2/ another signal which may attributed to photobleaching. The diffusion of resorufin from the inside to the outside of the vesicle is clearly observed on Figures 2 to 7 and is fast. On B, the mono-exponential fitting deviates from the signal from  $t \sim 25 \text{ s}$ , indicating that the signal between 0 and  $\sim 25 \text{ s}$  would correspond the fast diffusion of resorufin, whereas the slow decay from 25 s to 100 s would be due to photobleaching of the remaining entrapped resorufin.

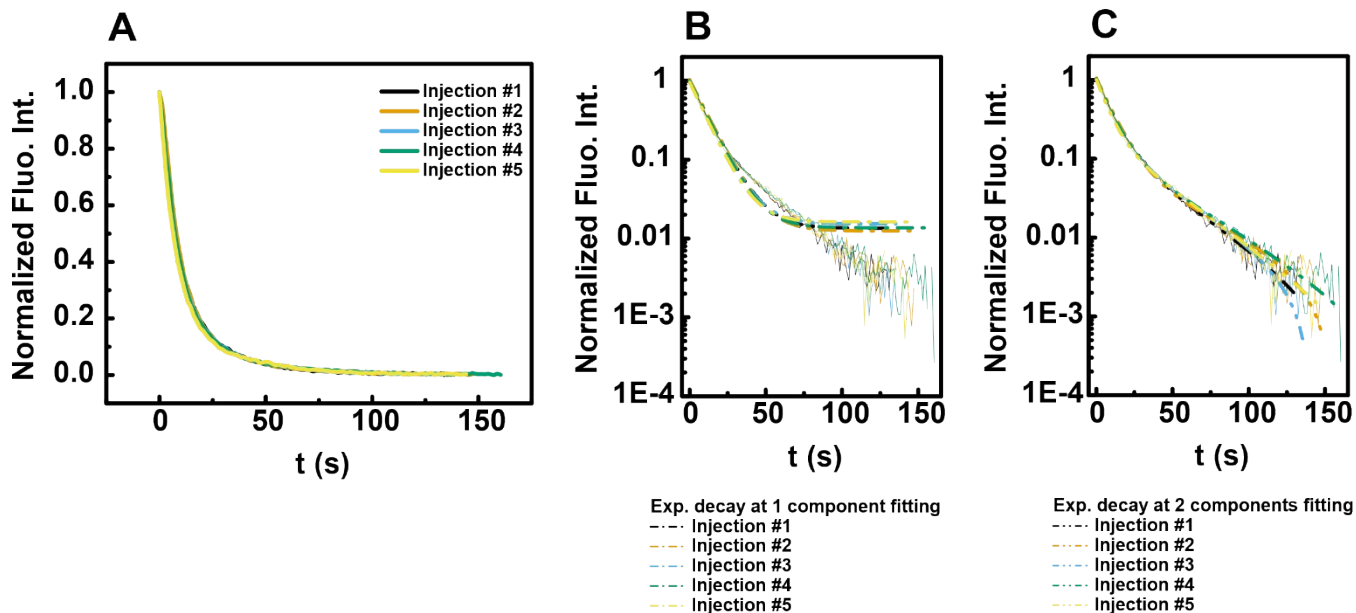


**Figure S8.** The signals of each injection from Figure 4 were normalized ([0;1]) and the x-axis was offset to  $t = 0$  for each injection (A). An exponential decay at 1 component fitting (B) and an exponential decay at 2 components fitting (C) were applied on each injection signal. B and C y-axis are in Log10. Solid lines represent the normalized fluorescence intensity of each injection. Dash-dot lines represent the exponential decay at 1 component fitting ( $y = A_1 \times \exp(-t/\tau_1) + y_0$ ). Dash-dot-dot lines represent the exponential decay at 2 components fitting ( $y = A_1 \times \exp(-t/\tau_1) + A_2 \times \exp(-t/\tau_2) + y_0$ ). As for Figure S7, the best fitting function of the signal is the 2-component exponential decay function illustrating the diffusion and potential photobleaching of resorufin. On B, the mono-exponential fitting deviates from the signal from  $t \sim 50$  s, indicating that the signal between 0 and  $\sim 50$  s would correspond the fast diffusion of resorufin, whereas the slow decay from 50 s to 150 s would be due to photobleaching of the remaining entrapped resorufin.

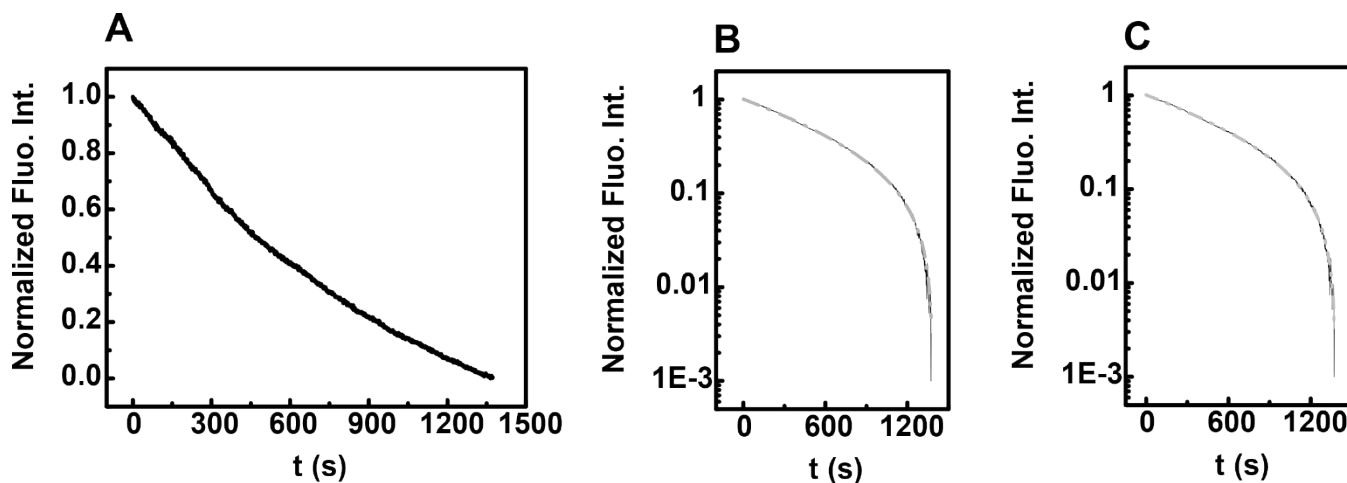


**Figure S9.** The signals of each injection from Figure 5 were normalized ([0;1]) and the x-axis was offset to  $t = 0$  for each injection (A). An exponential decay at 1 component fitting (B) and an exponential decay at 2 components fitting (C) were applied on each injection signal. B and C y-axis are in Log10. Solid lines represent the normalized fluorescence intensity of each injection. Dash-dot lines represent the exponential decay at 1 component fitting ( $y = A_1 \times \exp(-t/\tau_1) + y_0$ ). Dash-dot-dot lines represent the exponential decay at 2 components fitting ( $y = A_1 \times \exp(-t/\tau_1) + A_2 \times \exp(-t/\tau_2) + y_0$ ). In this case, there are no apparent differences

between the 1- or 2-component exponential decay fitting. Indeed, in this experiment, the production of resorufin is constant, as the diffusion. The production and diffusion rates are faster than the photobleaching rate, which is therefore not significant.

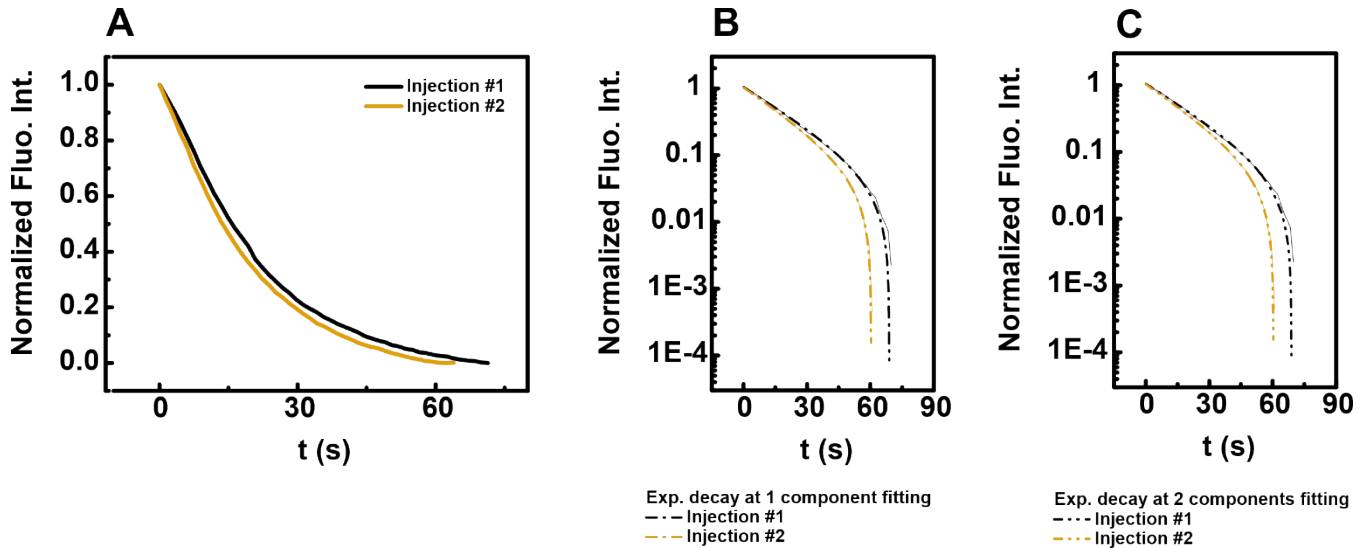


**Figure S10.** The signals of each injection from Figure 6 were normalized ([0;1]) and the x-axis was offset to  $t = 0$  for each injection (A). An exponential decay at 1 component fitting (B) and an exponential decay at 2 components fitting (C) were applied on each injection signal. B and C y-axis are in Log10. Solid lines represent the normalized fluorescence intensity of each injection. Dash-dot lines represent the exponential decay at 1 component fitting ( $y = A_1 \times \exp(-t/\tau_1) + y_0$ ). Dash-dot-dot lines represent the exponential decay at 2 components fitting ( $y = A_1 \times \exp(-t/\tau_1) + A_2 \times \exp(-t/\tau_2) + y_0$ ). There are no apparent differences between the 1- or 2-component exponential decay fitting. The production of resorufin is slower than on Figure S8. Here, resorufin is produced by the bi-enzymatic reaction where the kinetically limiting step was set to the first reaction converting glucose into hydrogen peroxide and gluconolactone, whereas Figure S8 shows solely the second (and faster) reaction converting Amplex Red and hydrogen peroxide into resorufin. The fluorescence intensity decay is limited by resorufin production, not by diffusion. In this case, photobleaching seems not to be significant enough to be detected.

## 5. Dependence on Amplex Red concentration of the bi-enzymatic reaction in GUVs

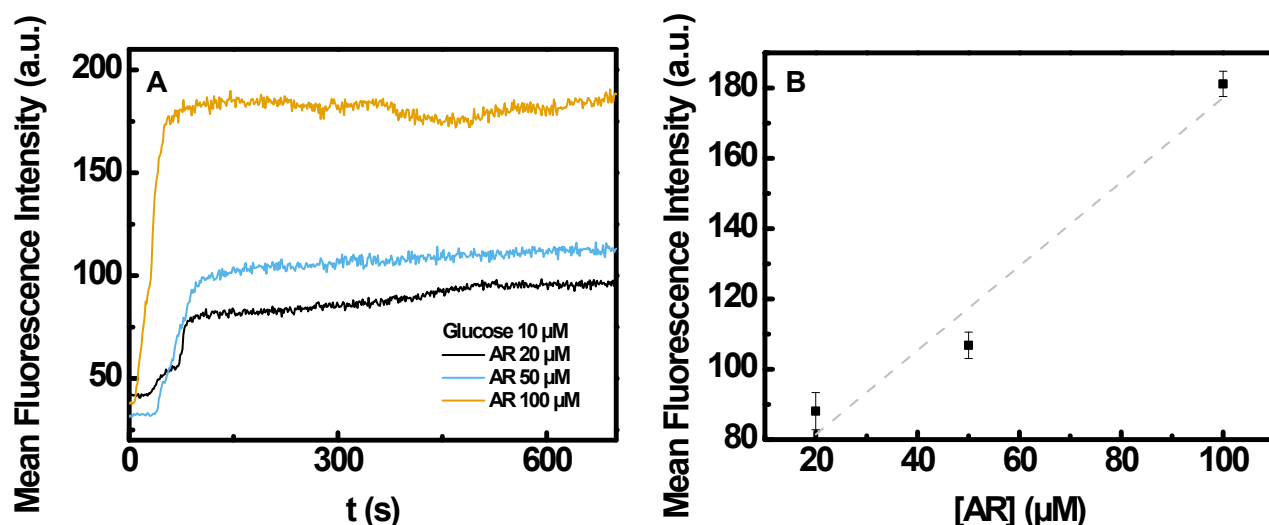


**Figure S11.** Dependence of the activity of the bi-enzymatic with Amplex Red concentration in GUVs. A. A glucose (10  $\mu\text{M}$ ) and AR (various concentrations)-containing GUV was injected once with a mix of GOx ( $4.4 \pm 0.4 \text{ U}\cdot\text{mL}^{-1}$  final) and HRP ( $0.35 \pm 0.03 \text{ U}\cdot\text{mL}^{-1}$  final). The resorufin production is reported by the mean fluorescence intensity inside the GUV over time detected by LSCM ( $\lambda_{\text{excitation}} = 514 \text{ nm}$  -  $\lambda_{\text{emission}} = 550\text{-}710 \text{ nm}$ ). Three concentrations of AR were tested (20, 50 and 100  $\mu\text{M}$ ), in three independent experiments. B. The average mean fluorescence intensity between 100 and 600 s is plotted in function of the AR concentration, showing an apparent linear dependence of the bi-enzymatic reaction activity with the substrate concentration when the experiment is performed in GUVs.

## 6. Volumes and concentrations calculations for each injection in each experiment

	GUV diameter ( $\mu\text{m}$ )	Volume ( $\mu\text{L}$ )	$\Delta V$ ( $\mu\text{L}$ )	[Resorufin] per inj. ( $\mu\text{M}$ )
Before injection	155	1949,82		
After injection	163	2267,57	317,76	0,35
Before injection	163	2267,57		
After injection	167	2438,64	171,07	0,18
Before injection	167	2438,64		
After injection	172	2664,31	225,66	0,21
Before injection	172	2664,31		
After injection	177	2903,48	239,17	0,21
			Average	0,24
			Std. Dev.	0,08

**Table S1.** Diameter measurements obtained from images before and after each injection presented on Figure 3. Volumes of the vesicle before and after each injection was calculated. By difference, the injected volume was determined, and the concentration of resorufin after each injection was estimated.

The resorufine diffusing outside of the vesicle almost immediately, those concentrations are theoretical concentrations based on the dilution of the stock solution in the pipette inside the volume of the vesicle. The average concentration of resorufin is given at the bottom of the table with the standard deviation.

	GUV diameter ( $\mu\text{m}$ )	Volume (pL)	$\Delta V$ (pL)	[AR] per inj. ( $\mu\text{M}$ )	[HRP] per inj. (U/mL)	[HRP] absolute (U/mL)
Before injection	143	1531,11				
After injection	146	1629,51	98,40	6,04	0,02	0,02
Before injection	146	1629,51				
After injection	151	1802,72	173,21	9,61	0,04	0,06
Before injection	151	1802,72				
After injection	153	1875,31	72,58	3,87	0,02	0,08
Before injection	153	1875,31				
After injection	155	1949,82	74,51	3,82	0,02	0,09
Before injection	155	1949,82				
After injection	161	2185,12	235,31	10,77	0,04	0,14
Average				6,82	0,03	
Std. Dev.				3,23	0,01	

**Table S2.** Diameter measurements obtained from images before and after each injection presented on Figure 4. Volumes of the vesicle before and after each injection was calculated. By difference, the injected volume ( $\Delta V$ ) was determined. The concentration of Amplex Red (AR) and the enzyme (HRP) after each injection was estimated. AR diffusing outside of the vesicle almost immediately, those concentrations are theoretical concentrations based on the dilution of the stock solution in the pipette inside the volume of the vesicle. The average concentration of AR and HRP is given at the bottom of the table with the standard deviation. HRP remaining sequestered inside the vesicle, the accumulated concentration of HRP over injections is given in the last column.

	GUV diameter ( $\mu\text{m}$ )	Volume (pL)	$\Delta V$ (pL)	[HRP] (U/mL)
Before injection	60	113,10		
After injection	90	381,70	268,61	0,28

**Table S3.** Diameter measurements obtained from images before and after injection presented on Figure 5. Volumes of the vesicle before and after injection was calculated. By difference, the injected volume ( $\Delta V$ ) was determined. The concentration of the enzyme (HRP) after injection was estimated.

	GUV diameter ( $\mu\text{m}$ )	Volume (pL)	$\Delta V$ (pL)	[AR] per inj. ( $\mu\text{M}$ )	[HRP] per inj. (U/mL)	[HRP] absolute (U/mL)
Before injection	138	1376,06				
After injection	170	2572,44	1196,39	46,51	0,19	0,19
Before injection	170	2572,44				
After injection	195	3882,42	1309,98	33,74	0,13	0,32
		Average		40,12	0,16	
		Std. Dev.		9,03	0,04	

**Table S4.** Diameter measurements obtained from images before and after each injection presented on Figure 6. Volumes of the vesicle before and after each injection was calculated. By difference, the injected volume ( $\Delta V$ ) was determined. The concentration of Amplex Red (AR) and the enzyme (HRP) after each injection was estimated. AR diffusing outside of the vesicle almost immediately, those concentrations are theoretical concentrations based on the dilution of the stock solution in the pipette inside the volume of the vesicle. The average concentration of AR and HRP is given at the bottom of the table with the standard deviation. HRP remaining sequestered inside the vesicle, the accumulated concentration of HRP over injections is given in the last column.

	GUV diameter ( $\mu\text{m}$ )	Volume (pL)	$\Delta V$ (pL)	[HRP] (U/mL)	[GOx] (U/mL)
Before injection	39	31,06			
After injection	108	659,58	628,52	0,38	4,76

**Table S5.** Diameter measurements obtained from images before and after injection presented on Figure 7. Volumes of the vesicle before and after injection was calculated. By difference, the injected volume ( $\Delta V$ ) was determined. The concentrations of enzymes (HRP and GOx) after injection were estimated.